Open Access **Baghdad Science Journal** **P-ISSN: 2078-8665**
2020, 17(2):488-493 **E-ISSN: 2411-7986**

1DOI: http://dx.doi.org/10.21123/bsj.2020.17.2.0488

A Theoretical Investigation on Chemical Bonding of the Bridged Hydride Triruthenium Cluster: [Ru_3 (μ-H)(μ_3-κ^2-Hamphox-*N*,*N*)$(CO)_9$]

Muhsen Abood Muhsen Al-Ibadi* ***Abrar Taha Tawfeeq Alkanabi*** ***Ahlam Hussein Hasan Duraid***

Received 20/11/2019, Accepted 12/2/2020, Published 1/6/2020

Abstract:

Ruthenium-Ruthenium and Ruthenium–ligand interactions in the triruthenium "[Ru_3(μ-H)(μ_3-κ^2-Hamphox-*N*,*N*)$(CO)_9$]" cluster are studied at DFT level of theory. The topological indices are evaluated in term of QTAIM (quantum theory of atoms in molecule). The computed topological parameters are in agreement with related transition metal complexes documented in the research papers. The QTAIM analysis of the bridged core part, i.e., Ru_3H, analysis shows that there is no bond path and bond critical point (chemical bonding) between Ru(2) and Ru(3). Nevertheless, a non-negligible delocalization index for this non-bonding interaction is calculated. The interaction in the core Ru_3H can be described as a (4centre–4electron) type. For Ru-N (oxazoline ring) bond, the calculated topological data propose a pure σ-bond. The computed topological parameters of oxazoline ligand reveal the presence of slightly some double bond characters within ligand ring.

Key words: Metal-metal bonds, QTAIM bonding analysis, Ruthenium cluster.

Introduction:

The properties of metal-metal interaction in clusters have been developed and widely studied as some important research dealt with the synthesis and characterization of the anionic complexes (1-5). Some were studies of cluster with low valent metal such as $Fe_2(CO)_9$, showed that the Fe-Fe separation was short enough to imply a M-M bond (6-11). The important development in the topological analysis, specifically, the atoms in molecules (AIM) theory which developed by Bader and his group, is to study both experimental and theoretical electron density distributions. Additionally, this approach provides a useful tool for studying various interactions in a molecular system(12-17).

In this paper, we aim to study the nature of the interactions between the various Ru–Ru metal atoms and Ru–ligand in mono hydride triruthenium clusters "[Ru_3(μ-H)(μ$_3$-κ^2-Hamphox-N,N)(CO)9] (H_2ox = H_2aminox)" (18), (Fig. 1), by applying QTAIM method. The Ru–Ru vectors are bridged by hydride ligands, rather than by the N-H group. In addition, one of the ruthenium atoms is attached to the N atom of the oxazoline ring.

Department of Chemistry, College of Science, University of Kufa, Najaf, Iraq.
*Corresponding author: muhsen.alibadi@uokufa.edu.iq
*ORCID ID: https://orcid.org/0000-0001-8639-4888

This would then offer a good opportunity to examine the topological features of different bonding interactions inside the cluster.

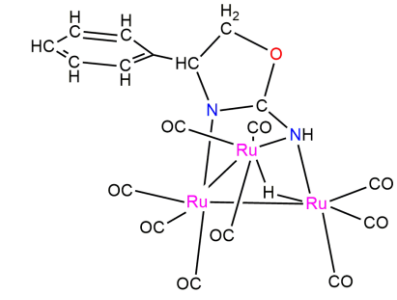

(i)

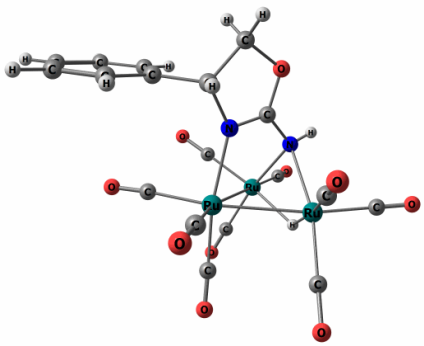

(ii)

Figure 1. (i) Two dimension structure and (ii) optimized structure of "[Ru_3(μ-H) (μ_3-κ^2-Hamphox-*N*,*N*) $(CO)_9$]"(18).

Baghdad Science Journal
P-ISSN: 2078-8665
E-ISSN: 2411-7986

Computational Methods:

The optimization of the cluster, where the *X-ray* diffraction structure was used as a starting point(18), was carried out using PBE1PBE functional as implemented in the GAUSSIAN09 (19). The LANL2DZ basis set (20) was applied for Ru and 6-31G(d,p) basis set for other atoms(21). The geometry optimization with no restrictions was carried out and stationary points were confirmed to be real minima by computation of its vibrational frequencies. The topological parameters of the optimized structure were computed with the PBE1PBE functional and WTBS basis set for Ru (22) and 6-31G (d, P)for other atoms using the AIM2000 programs (23).

Results and Discussion:

The topological analysis of the electron density offers a deep investigation of the nature of interactions in the clusters. A chemical bond, according to this analysis, is characterized by a line called bond path (bp) which binds the nuclei of two bonded atoms through a bond critical point (bcp). Fig. 2 shows the molecular graph of the cluster which was obtained by using the QTAIM method. In this Figure, the bond paths, bond and ring critical points have easily been observed. Interestingly, all Ru-Ru and Ru-ligand bcps and bps were exist except for the Ru(3) and Ru(2) interaction which was not observed. Also, five ring critical points(rcpt) corresponding to the N(1)-C(1)-O(1)-C(2)-C(3), C(4)-C(5)-C(6)-C(7)-C(8)-C(9), Ru(2)-N(2)-Ru(3)-H(1), Ru(1)-N(1)-C(1)-N(2)-Ru(2) and Ru(1)-Ru(2)-N(2)-Ru(3) were observed.

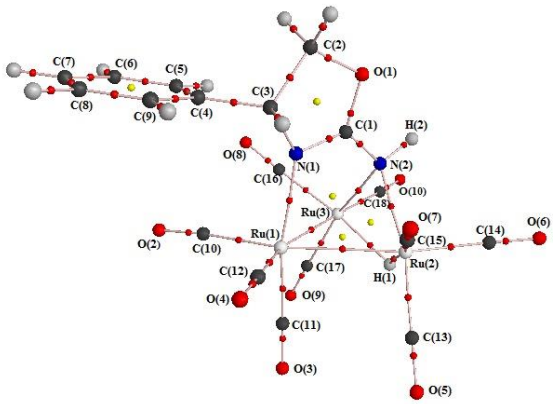

Figure 2. The molecular graph of the "[Ru_3(μ-H)(μ_3-κ^2-Hamphox-*N*,*N*)$(CO)_9$]" cluster (the bond paths, bond and ring critical points, which are shown as gray lines ,red and yellow circles, respectively).

Fig. 3 shows the a gradient map of the Ru_3H core, where the critical points positions in Ru(1)-Ru(2) and Ru(1)-Ru(3) interactions are indicated as well as the bond paths and its atomic basin. Conversely, the interaction between Ru(2) and Ru(3) the bps and bcps cannot be observed. In the same plane, the bps and bcps existed within both bridged ligand atoms (H(1) and N(2)) and Ru(2) and Ru(3) metals are also observed in the plot.

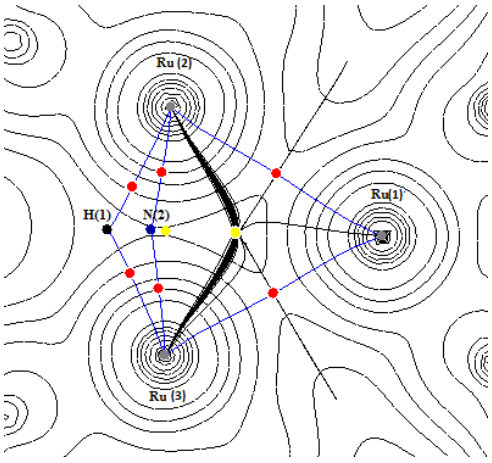

Figure 3. Gradient trajectories map through a hydride bridged triruthenium core plane (Ru(1), Ru(2) and Ru(3) are in plane whereas H(1) and N(2) are out of plane).

A gradient trajectory map of the NHC ring for the Hamphox ligand plane are presented in Fig. 4. It shows critical points and bond paths between attractors in the ligand ring. The bp and bcp of the interactions of the N(1) atom of the amino oxazoline ligand with Ru(1) atom was also found. Furthermore, all bps and bcps as well as rcps in the rings made between Ru(1)-N(1)-C(1)-N(2)- Ru(2 and 3) are also found.

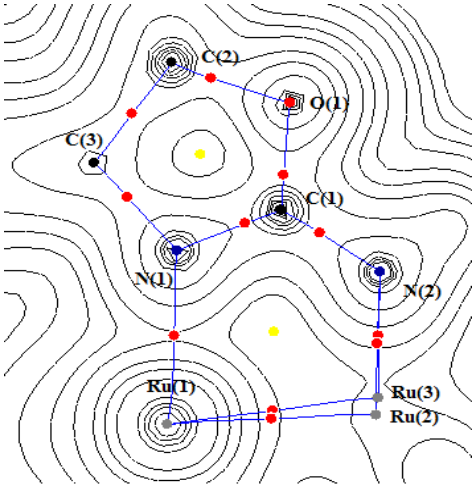

Figure 4. Gradient trajectories map through the plane of Hamphox ligand ring (Ru(1), N(1), C(1), O(1), C(2), C(3), and N(2) are in plane whereas Ru(2) and Ru(3) are out of plane)

Based on QTAIM, as presented in Table 1, the topological parameters for the cluster under study were studied.

Baghdad Science Journal
P-ISSN: 2078-8665
E-ISSN: 2411-7986

Table 1. Calculated QTAIM parameters of triruthenium cluster.

Bond	ρ_{BCP}	$\nabla^2\rho_{BCP}$	G_{BCP}	H_{BCP}	V_{BCP}	ε_{BCP}**
Ru(1)-Ru(2)	0.436	0.679	0.248	-0.079	-0.327	0.062
Ru(1)-Ru(3)	0. 442	0.684	0.252	-0.081	-0.333	0.054
Ru(1)-N(1)	0.784	3.895	1.053	-0.079	-1.132	0.070
Ru(2,3)-N(2)*	0.779	3.720	1.017	-0.093	-1.110	0.018
Ru(2,3)-H(1)*	0.765	1.796	0.671	-0.226	-0.897	0.071
N(1)-C(1)	3.853	-10.339	4.185	-6.770	-1.955	0.031
C(1)-O(1)	3.138	-3.426	4.159	-5.015	-9.174	0.038
C(2)-O(1)	2.389	-3.712	2.392	-3.320	-5.712	0.014
C(3)-C(2)	2.462	-5.720	0.556	-1.986	-2.542	0.044
C(3)-C(4)	2.584	-6.284	0.590	-2.161	-2.752	0.035
N(1)-C(3)	2.659	-7.452	1.238	-3.101	-4.340	0.027
N(2)-H(2)	3.411	-18.034	5.461	-0.140	-5.601	0.021
N(2)-C(1)	3.396	-12.713	1.831	-5.009	-6.840	0.014
Ru-C*	1.465	-1.291	1.563	-0.983	-2.546	0.042
C-O*	4.563	-2.998	10.489	-7.483	-17.973	0.001

*Average values.
** " (ρ_{BCP})electron density(eÅ^{-3}), ($\nabla^2\rho_{BCP}$) Laplacian of the electron density(eÅ^{-5}) (G_{BCP}) kinetic energy density ratio (he^{-1}), (V_{BCP}) potential energy density ratio (he^{-1}), (H_{BCP}) total energy density ratio and (ε_{BCP}) ellipticity."

In the Ru_3H core, as mentioned above, no bond path or bond critical point was found between the hydride-bridged Ru(2)…Ru(3) interaction. For Ru(1)-Ru(2) and Ru(1)-Ru(3) interactions, presented in Tab. 1, the calculated values of ρ_{BCP} are [0.436 and 0.442 eÅ^{-3}], respectively. Furthermore, the calculated Laplacian and Kinetic energy at the critical points of both bonds have small positive values, 0.679 eÅ^{-5}, 0.248 he^{-1} and 0.684 eÅ^{-5}, 0.252 he^{-1}, respectively, thus pointing out that both bonds have typical open-shell M-M interactions. Based on the computed ellipticity (ε_{BCP}), small values for both Ru(1)-Ru(2) and Ru(1)-Ru(3) bonds, 0.062 and 0.054, respectively, are comparable to those previously published for Ru-Ru and Os-Os bonds (24, 25). The electron density value (an average 0.765 eÅ^{-3}) and its Laplacian (an average 1.796 eÅ^{-5}) associated with the Ru(2,3)-H(1) bonds indicate that the strength of these bonds is in agreement with those reported in numerous other research for pure covalent single bonds(8). Moreover, the average values of the ellipticity of Ru-H bonds is (0.071), which is close to the calculated value for Ru-H (0.086) in the "[$Ru_3(\mu\text{-}H)_2(\mu^3\text{-}MeImCH)(CO)_9$]" cluster (26). The core part, shown in Fig. 5, can also be analysed by looking at the plot of the laplacian distribution of the cluster in the plain contain Ru(1)-Ru(2)-H(1)-Ru(3) part. In this plot, the Valence Shell Charge Concentration VSCC of the hydrogen bridge atom (H(1)) is polarized toward Ru(2)-Ru(3) edge.

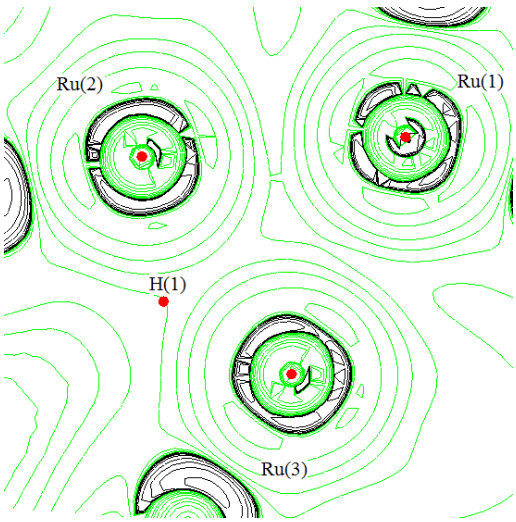

Figure 5. Plot of the Laplacian distribution in the triruthenium plane.

A lack of a bcp and bond path between Ru(2) and Ru(3) limit an interpretation of any interaction properties between them. Therefore, to give more insight to this interaction, and also to Ru(1)-Ru(2,3) bonds, we calculated the delocalisation index δ(A,B) (27) which is a measure of the number of shared electrons. This index is an appropriate indicator of the interaction that does not depend on the presence of bond critical point.

The numerical results in Table 2, show that the calculated delocalization indices of the Ru(1)-Ru(2,3) bonds are 0.487 and 0.500, respectively. The results obtained are in agreement with the calculated delocalization indices for the M-M bonds(25, 28, 29). In contrast, the value of delocalization indices for nonbonding Ru(2)...Ru(3) is 0.202, which is in excellent agreement with

computed bridged-hydride Metal...Metal nonbonding interactions(25).

Table 2. Calculated delocalization indices δ(A, B) of cluster.

atom pairs	δ_{AB}	atom pairs	δ_{AB}**
Ru(1)-Ru(3)	0.500	N(2)-C(1)	0.846
Ru(1)-Ru(2)	0.487	Ru-CO *	1.103
Ru(2,3)-H(1)*	0.455	C-O *	1.520
Ru(2,3)-N(2)*	0.507	Ru(2)...Ru(3)	0.202
Ru(1)-N(1)	0.510	Ru(2,3)…C(1)*	0.019
N(1)-C(1)	1.050	Ru(2,3)…H(2)*	0.011
C(1)-O(1)	0.778	Ru(1)...C(1)	0.023
C(2) -O(1)	0.079	Ru(1)...C(3)	0.027
C(2)-C(3)	0.008	Ru(2,3)…N(1)*	0.035
C(3)-N(1)	0.852	Ru(1)…N(2)	0.040
N(2)-H(2)	0.737	Ru…O_{CO} *	0.192

*Average values.
** (δ_{AB}) delocalisation indices

As seen in Table 2, the average value of the calculated Ru-H delocalization index is 0.455, and is close to that computed by Cabeza *et al*(26) for the Ru–H bonds in the "$[Ru_3(\mu\text{-}H)_2(\mu^3\text{-}MeImCH)(CO)_9]$" cluster (0.474). Furthermore, the results obtained are in agreement with the few cases calculated for the M-H interactions(30). As it is expected, these data pointed out that the number of shared electron in the Ru-H bond is a half electron pair. Interestingly, comparing the data in Table (1) and Table (2) shows that the delocalisation index for Ru(1)-Ru(2,3) bonds is quite similar, whereas the topological parameters for these bonds show remarkable differences. The most significant observation is that the number of electron pairs in the Ru(1)-Ru(2)-H(1)-Ru(3) core is 2.1 electron pairs (summation of bonding and non-bonding delocalization indices). Our results indicate that a multicentre 4c-4e interaction exists in the bridged core parts.

The calculated values of topological properties of the Ru-CO bonds are depicted in Table 1 and are in line with the literature(30). Our results indicate that the average value of ρ_{BCP} for Ru-CO bonds (1.465 $Å^{-3}$) are significantly higher than Ru-Ru bonds and are lower than the calculated value for covalent bonds between non-metal atoms. By reasons of π- back donation, that contains the M...O_{CO} interaction, the computed delocalization indices have been taken as a proof for the existing of π-back bonding in Metal-CO bonds(31, 32). For the same reason, the M...O_{CO} delocalization indices were calculated, see Table 2.

In consequence, the calculated value of δ(Ru...O_{CO}) (in average 0.192) is found comparable to δ(M...O_{CO}) for other metals such as Co, Ni, Fe, Ru and Os carbonyl complexes (with the range 0.15-0.25)(29-31) ,in which a π-back donation was observed. By contrast, the values are between (0.04 and 0.09) for H_3BCO and $[Cu(CO)_2]^+$, respectively, due to the absence of π-back bonding(31).

The six topological parameters in Table (1), i.e. ρ_{BCP}, $\nabla^2\rho_{BCP}$, G_{BCP}, H_{BCP}, V_{BCP} and ε_{BCP}, show high similarities for both (1)-N(1) and Ru(2,3)-N(2) bonds. Importantly, the calculated ellipticity (ε_{BCP}) of Ru(1)-N(1) (0.070) is higher than the ellipticity of Ru(2,3)-N(2) (0.018) indicating that the former bond has a marginally greater double bond features. From Table 2, the calculated delocalization indexes for both Ru(2,3)-N(2) and Ru(1)-N(1) bonds are around 0.51. This indicates that the number of electron pair shared is 0.5. Fig. 6 shows the distortion in VSCCs for both nitrogen atoms in which linked to ruthenium metal atoms.

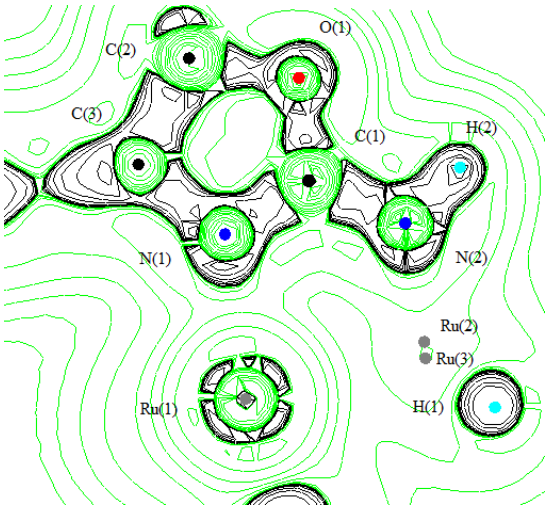

Figure 6. Laplacian map through Ru-oxazolen ring.

In a similar manner for Ru-CO calculations, the Ru(1,2,3)…C(1,3) delocalization indices were computed in order to confirm the existence or absence of π bonding in the Ru(1,2,3)-N(1,2) as presented in Table 2. Depending on small and nearly equal values in Table 2, one can conclude that there is no π-bonding features between Ru and oxazoline but only pure σ-donor.

The trajectory map of the oxazoline ring ligand (the bcps, bps and atomic basins), which is presented in Fig.4, shows an interesting point. The bcps is shifted toward the less electronegative atoms, i.e. C(1,2,3). The topological values of O(1)-C(1,2) and N(1,2)-C(1) pointed out that, those bonds have a slightly double bond characters.

Conclusion:

The interactions in the triruthenium "$[Ru_3(\mu\text{-}H)(\mu_3\text{-}\kappa^2\text{-}Hamphox\text{-}N,N)(CO)_9]$" cluster are explored by means of using topological indices derived from the QTAIM analysis. The AIM

analyses of the bridged core part Ru_3H reveal the absence of a bond critical point and bond path in the Ru(2)…Ru(3) interaction. According to our calculations, the bridged core part a 4c–4e type is suggested to exist. The topological analysis of the Ru-N bond confirms the presence of σ-bond. The AIM analyses of the calculated topological indices of the oxazoline ligand suggest a substantial degree of π-electron delocalization within the ligand rings. The topological results for Ru–Ru and Ru–ligand bonds are comparable with those previously found for other compounds such as Fe, Co, Ni, Ru and Os, carbonyl complexes.

Authors' declaration:

- Conflicts of Interest: None.
- We hereby confirm that all the Figures and Tables in the manuscript are mine ours. Besides, the Figures and images, which are not mine ours, have been given the permission for re-publication attached with the manuscript.
- Ethical Clearance: The project was approved by the local ethical committee in University of Kufa.

References:

1. Cotton F, Harris C. The Crystal and Molecular Structure of Dipotassium Octachlorodirhenate(III) Dihydrate, K2[Re2Cl8]2H2O. Inorg Chem. 1965;4(3):330-333.
2. Rosemann NW, Eußner JP, Dornsiepen E, Chatterjee S, Dehnen S. Organotetrel Chalcogenide Clusters: Between Strong Second-Harmonic and White-Light Continuum Generation. J. Am. Chem. Soc. 2016; 138 : 16224 —16227
3. Rinn N, Guggolz L, Gries K, Volz K, Senker J, Dehnen S. Formation and Structural Diversity of Organo-Functionalized Tin-Silver Selenide Clusters. Chem–Eur. J. 2017; 23: 15607 —15611
4. Hanau K, Rinn N, Argentari M, Dehnen S. Organotin Selenide Clusters and Hybrid Capsules. Chem.–Eur. J. 2018; 24:11711 —11716
5. Engel A, Dornsiepen E, Dehnen S. Click reactions and intramolecular condensation reactions on azido-adamantyl-functionalized tin sulfide clusters. Inorg. Chem. Front. 2019; 6 : 1973 —1976.
6. Farrugia LJ, Senn HM. Metal-Metal and metal-ligand bonding at a QTAIM catastrophe: A combined experimental and theoretical charge density study on the alkylidyne cluster Fe3(μ-H)(μ-COMe)(CO)10. J Phys Chem A. 2010;114(51):13418-13433.
7. Santner S, Heine J, Dehnen S. Synthesis of Crystalline Chalcogenides in Ionic Liquids. Angew. Chem. Int. Ed. 2016; 55 : 876 —893
8. Wen G H, Zhang R F, Li Q L, Zhang S L, Ru J, Du J Y, et al. Synthesis, structure and in vitro cytostatic activity study of the novel organotin(IV) derivatives of p-aminobenzenesulfonic acid. J. Organomet. Chem. 2018; 861 :151 —158.
9. Engel A, Dehnen S. Amino Acid Functionalized Organotin Trichlorides and Their Tin Sulfide Clusters. Eur. J. Inorg. Chem. 2019 Oct 31;2019 (39-40):4313-20.
10. Manos MJ, Kanatzidis MG. Metal sulfide ion exchangers: superior sorbents for the capture of toxic and nuclear waste-related metal ions. Chem. Sci. 2016;7(8):4804-24.
11. Berndt JP, Engel A, Hrdina R, Dehnen S, Schreiner PR. Azido-Adamantyl Tin Sulfide Clusters for Bioconjugation. Organometallics. 2018 Dec 21;38(2):329-35.
12. Bader RFW. A Bond Path: A Universal Indicator of Bonded Interactions. J Phys Chem A. 1998;102:7314–7323. doi:10.1021/jp981794v
13. Macchi P. The future of topological analysis in experimental charge-density research. Acta Crystallogr. B Struct. Sci. Cryst. Eng. Mater. 2017 Jun 1;73(3):330-6.
14. Macchi P, Gillet JM, Taulelle F, Campo J, Claiser N, Lecomte C. Modelling the experimental electron density: only the synergy of various approaches can tackle the new challenges. IUCrJ. 2015 Jul 1;2(4):441-51.
15. Tolborg K, Iversen BB. Electron Density Studies in Materials Research. Chem. Eur. J. 2019 Nov 27;25(66):15010-29.
16. Rahm M, Zeng T, Hoffmann R. Electronegativity Seen as the Ground-State Average Valence Electron Binding Energy. J. Am. Chem. Soc. 2018 Nov 30;141(1):342-51.
17. Sasaki T, Kasai H, Nishibori E. Tightly binding valence electron in aluminum observed through X-ray charge density study.Sci. Rep. 2018 Aug 10;8(1):1-7.
18. Cabeza JA, Da Silva I, Del Río I, Gossage RA, Miguel D, Suárez M. Triruthenium carbonyl clusters derived from chiral aminooxazolines: synthesis and catalytic activity. Dalton Trans. 2006;3(20):2450-2455.
19. Frisch MJ, Trucks GW, Schlegel HB, Scuseria GE, Robb MA, Cheeseman JR, et al. Gaussian 09, Revision D. 2009;1.
20. Wadt WR, Hay PJ. Ab initio effective core potentials for molecular calculations. Potentials for main group elements Na to Bi. J Chem Phys. 1985;82(1):284-298.
21. Hehre WJ, Ditchfield R, Pople JA. Self—consistent molecular orbital methods. XII. further extensions of Gaussian—type basis sets for use in molecular orbital studies of organic molecules. J Chem Phys. 1972;56(5):2257-2261.
22. Adamo C, Barone V. Toward reliable density functional methods without adjustable parameters: The PBE0 model. J Chem Phys. 1999;110(13):6158.
23. Biegler-König F, Schönbohm J. Update of the AIM2000-program for atoms in molecules. J. comput. Chem. 2002; 23(15):1489.
24. Gervasio G, Bianchi R, Marabello D. Unexpected intramolecular interactions in $Ru_3(CO)_{12}$: An experimental charge density study at 120 K. Chem Phys Lett. 2005;407(1-3):18-22.

25. Van der Maelen JF, García-Granda S, Cabeza JA. Theoretical topological analysis of the electron density in a series of triosmium carbonyl clusters: $[Os_3(CO)_{12}]$, $[Os_3(\mu\text{-}H)_2(CO)_{10}]$, $[Os_3(\mu\text{-}H)(\mu\text{-}OH)(CO)_{10}]$ and $[Os_3(\mu\text{-}H)(\mu\text{-}Cl)(CO)_{10}]$. Comput Theor Chem. 2011;968(1-3):55-63.
26. Cabeza JA, Van der Maelen JF, García-Granda S. Topological Analysis of the Electron Density in the N-Heterocyclic Carbene Triruthenium Cluster $[Ru_3(\mu\text{-}H)\ 2(\mu^3\text{-}MeImCH)(CO)_9]$ (Me 2 Im = 1,3-dimethylimidazol-2-ylidene). Organometallics. 2009;28(13):3666-3672.
27. Bader R, Stephens M. Spatial localization of the electronic pair and number distributions in molecules. J Am Chem, 1975;97(26):7391-7399.
28. Gatti C. Chemical bonding in crystals: new directions. Zeitschrift für Krist. 2005;220(5-6-2005):399-457.
29. Alhimidi SRH, Al-Ibadi MAM, Hasan AH, Taha A. The QTAIM Approach to Chemical Bonding in Triruthenium Carbonyl Cluster: $[Ru_3(\mu\text{-}H)(\mu^3\text{-}\kappa^2\text{-}Haminox\text{-}N,N)(CO)9]$. Journal of Physics. 2018, 1032, 012068.
30. Macchi P, Donghi D, Sironi A. The electron density of bridging hydrides observed via experimental and theoretical investigations on $[Cr_2(\mu^2\text{-}H)(Co)_{10}]^-$. J Am Chem Soc. 2005;127(47):16494-16504.
31. Al-Ibadi MA, Alkurbasy NE, Alhimidi SR. The topological classification of the bonding in [(Cp'Ru) 2 (Cp'Os)(μ3-N) 2 (μ-H) 3] cluster. InAIP Conference Proceedings 2019 Aug 22 (Vol. 2144, No. 1, p. 020009). AIP Publishing LLC.
32. Al-Ibadi MA, Oraibi DT, Hasan AH. The ruthenium–ruthenium bonding in bridged ligand system: QTAIM study of [Ru3 (μ3-κ2-MeImCH)(μ-CO)(CO) 9] complex. InAIP Conference Proceedings 2019 Aug 22 (Vol. 2144, No. 1, p. 020008). AIP Publishing LLC.

دراسة نظرية حول الترابط الكيميائي للمركب الجسري هيدريد ثلاثي روثينيوم العنقودي $[Ru_3(\mu\text{-}H)(\mu^3\text{-}\kappa^2\text{-}Hamphox\text{-}N,N)(CO)_9]$

محسن عبود محسن العبادي **ابرار طه** **احلام حسين حسن** **دريد توفيق الكنبي**

قسم الكيمياء، كلية العلوم، جامعة الكوفة، النجف، العراق.

الخلاصة:

تمت دراسة تأثرات الروثينيوم - الروثينيوم والروثينيوم - ليكاند في المركب العنقودي ثلاثي الروثينيوم $[Ru_3(\mu\text{-}H)(\mu^3\text{-}\kappa^2\text{-}Hamphox\text{-}N,N)(CO)_9]$ باستخدام نظرية دالة الكثافة. وتم تقييم المؤشرات التوبولوجية باستخدام QTAIM (نظرية الكم للذرات في الجزيء). المعلمات التوبولوجية المحسوبة تتفق مع معقدات المعادن الانتقالية ذات الصلة والموثقة في الأدبيات. دلت نتائج تحليلات QTAIM على غياب الروابط او النقاط الحرجة بين Ru(2)و Ru(3) للمركز Ru_3H. على الرغم من ذلك، تم حساب معامل عدم التمركز لهذا التأثر غير مرتبط. يمكن وصف التأثر الموجود في Ru_3H الأساسي بكونه من نوع رباعي المركز رباعي الالكترون (4C-4e). وبالنسبة لتاصر Ru-N (حلقة الأوكسازولين)، تقترح البيانات التوبولوجية المحسوبة ان نوع الأصرة هو سكما. وتكشف المعلمات التوبولوجية المحسوبة في ليكاند الأوكسازولين عن وجود بعض الروابط المزدوجة داخل حلقة الليكاند).

الكلمات المفتاحية: الروثينيوم العنقودي، اصرة معدن-معدن، تحليل التاصر QTAIM.